Parameter optimization and test of hydraulic soil insertion device of orchard gas explosion subsoiling and fertilizing machine

Congju Shen[1,2,3], Lixin Zhang[1,3*], Shouxing Jia[2,3], Yan Zhou[2,3], Fan Li[2], Yameng Dai[2], Jing Zhang[2], Wenxiao Ma[1]

(1. *College of Mechanical and Electrical Engineering, Shihezi University, Shihezi 832000, Xinjiang, China*;
2. *Xinjiang Academy of Agricultural and Reclamation Science, Shihezi 832000, Xinjiang, China*;
3. *Key Laboratory of Northwest Agricultural Equipment of Ministry of Agriculture and Rural Affairs, Shihezi 832000, Xinjiang, China*)

Abstract: Hydraulic soil insertion device is a key component of orchard gas explosion subsoiling and fertilizing machine to realize rod fixed point soil insertion and gas fertilizer injection into soil. In order to explore the influence of the main working parameters and structural parameters on the depth and cylinder pressure of the hydraulic insertion device during the insertion process, the working parameters were optimized to ensure the insertion quality and efficiency. In this paper, force analysis was performed on the rod insertion process, and key parameter equation of soil insertion resistance was established. LS-DYNA finite element simulation software was applied to analyze the force variation of the rod during the insertion process. Box-Behnken test optimization design method and Design-Expert V8.0.6.1 software were used to carry out parameter optimization test of hydraulic insertion device. A multivariate quadratic polynomial regression equation was established by setting the engine revolution, insertion rod diameter and insertion time as independent variables, and the operation parameters of the hydraulic insertion device were optimized based on the relationship between the independent variables and the response values. The results showed that the regression equation model based on the response values of insertion depth and cylinder pressure had a good fitting degree. The engine revolution, rod diameter and insertion time all had significant effects on the increase of insertion depth and decrease of cylinder pressure, with interaction between the engine speed and insertion time with the insertion depth, and interaction between any two factors of engine revolution, rod diameter and insertion time with the cylinder pressure. The influences of the test factors on the insertion depth showed a descending order as engine speed, insertion time, and rod diameter. The influences of the test factors on the cylinder pressure showed a descending order as engine speed, rod diameter, and insertion time. Based on the results of insertion depth and cylinder pressure, the optimal combination of parameters was as follows: engine revolution of 1450 r/min; rod diameter of 32 mm; and the insertion time of 8 s. Under this optimal combination, the insertion depth of the hydraulic insertion device was 44.43 cm, and the cylinder pressure was 23.09 MPa. The experimental results showed that the optimal combination of parameters could meet the agronomic requirements of fast and deep insertion, thus providing a theoretical support for the improvement and optimization of hydraulic soil insertion device of gas explosion subsoiling and fertilizing machine.

Keywords: orchard management machinery, subsoiling, gas explosion, fertilization, hydraulic insertion, optimization
DOI: 10.25165/j.ijabe.20231602.7126

Citation: Shen C J, Zhang L X, Jia S X, Zhou Y, Li F, Dai Y M, et al. Parameter optimization and test of hydraulic soil insertion device of orchard gas explosion subsoiling and fertilizing machine. Int J Agric & Biol Eng, 2023; 16(2): 132–141.

1 Introduction

Orchard subsoiling and topdressing is a key soil management process during growth period of fruit trees[1]. With the advancement of whole course mechanization of standardized orchards, higher requirements for subsoiling and topdressing technology were rendered. Insufficient subsoiling would thicken the plow pan or harden layer and destroy the permeability of soil, hindering the penetration of water, fertilizer and gas into the deep soil under the plow pan (harden layer). As a result, the fruit roots have to stay at the shallow plough layer, and the fruit trees would have low resistance to stress and would easily contract chlorosis and other diseases, or even have dead branches or die when encountering drought, waterlogging and freezing. Besides, as a perennial economic crop, fruit trees usually have deep roots, which normally require deep fertilization. Walnut and pear trees, for instance, require a fertilization depth of 40-60 cm[2,3], and the roots should not be damaged during fertilization. It's hard for conventional mechanical ditching fertilizer and pit fertilizer to meet the above requirements[4-7]. However, artificial digging for topdressing featured high labor intensity, low working efficiency and high labor cost, which is not suitable for large-scale cultivated orchards[8,9].

Orchard gas explosion subsoiling and fertilizing machine is a no-till subsoiling and fertilizing equipment that realizes deep soil

Received date: 2021-10-13 **Accepted date:** 2023-02-27
Biographies: Congju Shen, PhD candidate, Associate Researcher, research interest: agricultural engineering technology, Email: shencongju@163.com; **Shouxing Jia**, Researcher, research interest: agricultural engineering technology, Email: jia-shouxing@163.com; **Yan Zhou**, Researcher, research interest: orchard machinery, Email: 806551889@qq.com; **Fan Li**, Research Associate, research interest: orchard machinery, Email: 784313261@qq.com; **Yameng Dai**, Associate Researcher, research interest: orchard machinery, Email: 348093948@qq.com; **Jing Zhang**, Associate Researcher, research interest: orchard machinery, Email: 491848971@qq.com; **Wenxiao Ma**, MS candidate, research interest: agricultural engineering technology, Email: 582628621@qq.com.
***Corresponding author: Lixin Zhang**, PhD, Professor, research interest: mechanical engineering. College of Mechanical Electrical Engineering, Shihezi University, Shihezi 832000, Xinjiang, China. Tel: +86-17709939016, Email: zhlx2001730@126.com.

insertion, gas explosion subsoiling and gas fertilizer injection through soil insertion device[10]. Driven by hydraulic cylinder, the soil insertion device vertically inserts a steel cylindrical hollow slender rod into the soil at least 40 cm deep to convert gas and fertilizer into the soil via the inner cavity of the rod. MAC Engineering Corporation developed a small hand-hold soil improvement device for gas explosion injection of solid granular fertilizer[11,12]. This device adopted hydraulic driven linkage mechanism. But tests showed that the device is not suitable for soil environment in China. When applied in soil with hardness (hardness) higher than 2 MPa, the insertion rod has difficulty penetrating into the soil due to the light weight of the machine, even if increasing the working pressure of the hydraulic cylinder. Xi et al.[13,14] designed a tractor rear suspension orchard gas explosion subsoiling and fertilizing machine. This machine is applicable for the injection of liquid fertilizer, which pushes the drill pipe vertically into soil through gas hammer excitation and hydraulic force. The oil-cylinder piston pole is directly connected with the upper drill pipe. The two moved vertically in sync during the drilling process. The cylinder stroke has a linear relationship with the insertion depth. As the maximum depth reaches 50 cm, the insertion mechanism has a great longitudinal height due to the long cylinder stroke, restricting the operation of the machine in high-density orchards. Zhou et al.[15] designed a cam-driven punching mechanism suitable for liquid fertilizer injection in field crops.

In view of the above problems and based on the self-propelled caterpillar orchard gas explosion subsoiling and fertilizing machine[10,16], this paper performed further force analysis and LS-DYNA finite element simulation on the rod insertion process of double cylinder driven hydraulic insertion device, and analyzed the rod insertion and the change rules. Then Box-Behnken test optimization design method was used to carry out parameter optimization test. The impacts of the three parameters of engine revolution, rod diameter and insertion time on the insertion depth and cylinder pressure were studied, and the optimal combination of working parameters of the hydraulic insertion machine under experimental condition was established to ensure the working quality and insertion efficiency, thus providing theoretical support for the improvement and optimization of hydraulic soil insertion device of gas explosion subsoiling and fertilizing machine.

2 Structure and working principle

2.1 Structure of hydraulic soil insertion device

The structure of hydraulic soil insertion device is shown as Figure 1. As shown, the insertion device mainly consists of the hydraulic cylinder, rocker, lifting crank, guide assembly, slide rail mechanism, drilling rod, fixed hinge support and other components.

2.2 Working principle

Orchard gas explosion subsoiling and fertilizing machine applies a fixed point soil insertion operation mode for subsoiling and fertilization[10]. The hydraulic insertion device adopts an offset slider crank mechanism and a double cylinder driven execution unit, and transfers power through the lifting crank, rocker and guide assembly to realize the insertion and lifting of the insertion rod.

The soil insertion process is shown as Figure 2. As the driver drives the gas explosion subsoiling and fertilizing machine to the fertilizing point and switches the “insert/lift” handle on the control panel to “insert”, the hydraulic oil would flow into hole P (head port), pushing the piston pole of the cylinder to lengthen. Then the double cylinder piston pole drives the lifting crank with the guide assembly to roll down along the slideway of the slide mechanism

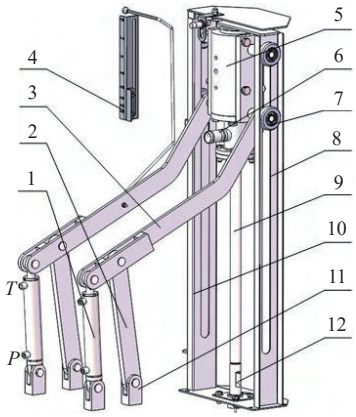

1. Hydraulic cylinder 2. Rocker 3. Lifting crank 4. Scale plate 5. Hammering device 6. Gas and fertilizer connector 7. Guide assembly 8. Slide rail mechanism 9. Drilling rod 10. Slide rack 11. Fixed hinge support 12. Gas fertilizer hole
Note: P is the oil inlet of head port, T is the oil inlet of rod port.

Figure 1 Structure of hydraulic soil insertion device

and brings the insertion rod to move vertically downward, thus initiating the drilling process. During the drilling process, the drilling depth can be observed with a scaleplate. Stop the drilling when the depth reaches the required insertion depth. Upon the completion of gas explosion subsoiling and fertilizing, the driver switches the “insert/lift” handle to “lift”, and the hydraulic would flow into hole T (rod port), driving the piston pole of the cylinder to retract. Then the double cylinder piston pole drives the lifting crank with the guide assembly to roll up along the slideway of the slide mechanism and brings the insertion rod to move vertically upward, thus initiating the lifting process. Stop the lifting when the insertion rod reaches the position as shown in Figure 2. The completion of the drilling and lifting process means a whole process of insertion, subsoiling and fertilizing operation was completed. The operation console instruction of the machine is shown in Figure 3.

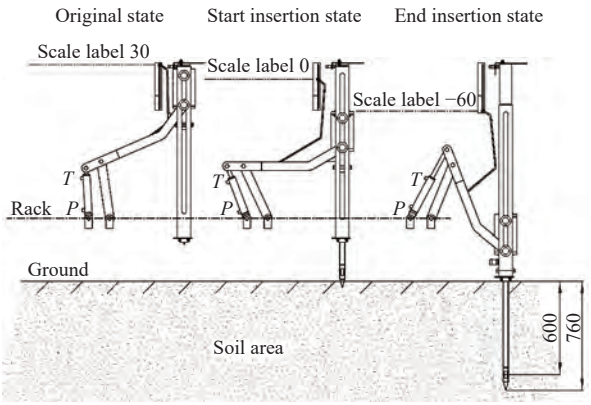

Figure 2 Soil insertion process of hydraulic soil insertion device

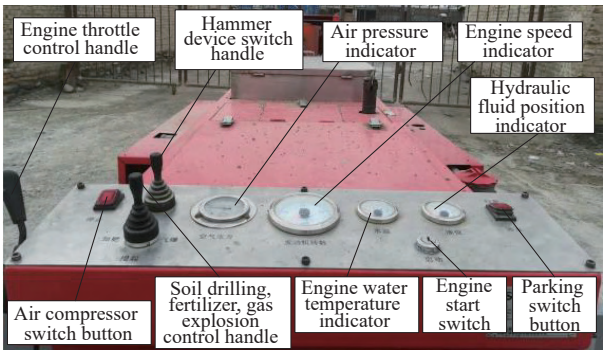

Figure 3 Operation console instruction

3 Hydraulic system design and component selection

3.1 Design of hydraulic system

The hydraulic system circuit of the soil insertion device is shown as Figure 4. The device adopted double cylinder drive and solenoid valve control mode. Quantitative gear pump was used for the hydraulic pump to convert the mechanical energy of the engine of the gas explosion subsoiling and fertilizing machine into hydraulic energy, which was then transmitted via hydraulic oil to the three-position four-way electromagnetic reversing valve to synchronously control the stroke of the two parallel cylinders installed at both sides, thus enabling the synchronous stretching of the two cylinders and controlling the drilling and lifting process of the insertion device.

As the two solenoid valves at the two sides of the reversing valve was powered off, the reversing valve was in meso-position function, the hydraulic oil would flow back to the oil tank, and the two cylinders would keep the piston pole of the cylinder locked through the two-way self-locking valve to ensure security. When the left solenoid valve was powered on, the hydraulic oil would flow into the head port (left port) of the two oil cylinders, and the cylinder piston pole would stretch out, thus initiating the drilling process; when the right solenoid valve was powered on, the hydraulic oil would flow into the rod port (right port) of the two oil cylinders, and the cylinder piston pole would retract, thus initiating the lifting process.

For exceptional operating case when the cylinder working pressure exceeded rated pressure, the overflow valve would open to relieve pressure to stabilize the circuit pressure and protect the hydraulic components. Meanwhile, oil suction filter is required for the hydraulic circuit to ensure clean hydraulic oil.

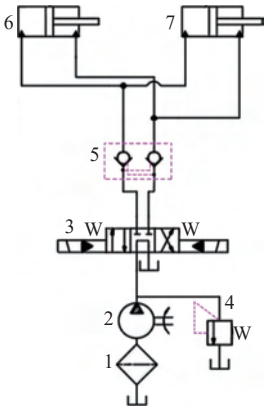

1. Filter 2. Metering pump 3. Solenoid directionalvalve
4. Overflow valve 5. Self-locking valve 6. Left oil cylinder
7. Right oil cylinder

Figure 4 Hydraulic system circuit of the soil insertion device

3.2 Selection of hydraulic components

Based on the design requirements of the hydraulic system of gas explosion subsoiling and fertilizing machine, the following components (Table 1) were selected for the hydraulic system of the soil insertion device.

Table 1 Hydraulic system components

Component	Model	Parameter
Gear pump	CBN-F306-LBR-YTJH	Rated revolution, 1500 r/min; Displacement, 6 mL/r; Rated pressure, 20 MPa (maximum 25 MPa); Volumetric efficiency ≥90%
Oil cylinder×2	Double-acting single piston type HSGL01-40/dE	Cylinder diameter, 40 mm; Rod diameter, 25 mm; Stroke, 200 mm
Solenoid directional valve	DSG-01-3C60-D12	Nominal diameter, 6 mm; Power, 12 V DC; Maximum flow, 63 L/min; Maximum working pressure, 31.5 MPa
Overflow valve	DBC-1-30B/315	Nominal diameter, 30 mm; Maximum flow, 600 L/min; Maximum regulating pressure, 31.5 MPa
Self-locking valve	SYS-L15H4	Nominal diameter, 15 mm; Nominal pressure, 31.5 MPa; Rated flow, 80 L/min
Filter	CFFA-250×120	Nominal flow, 120 L/min; Filter precision, 80 μm; Original pressure loss, 0.01 MPa

4 Force and simulation analysis of the insertion rod during soil insertion process

4.1 Force analysis of the insertion rod during soil insertion process

The force analysis of the insertion rod is shown as Figure 5. The acting forces of the insertion rod during the insertion process include: System external force on the rod F_w (kN), Positive pressure acting on the rod cylinder face P_f (kPa), Friction on the rod cylinder face F_f (kN), Positive pressure acting on the rod cone face P_n (kPa), and Friction on the rod cone face F_n (kN).

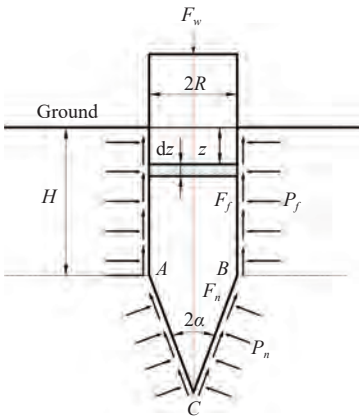

Figure 5 Forces acting on the insertion rod

Based on Rankine's earth pressure theory[17], integral method was used to solve the friction on the cylinder face of the insertion rod[13], and the combined soil frictional force on the cylinder face F_f (kN) was:

$$F_f = \int_0^H \mathrm{d}F_f = 2\mu\pi RK_0\gamma \int_0^H z\mathrm{d}z = \mu\pi RK_0\gamma H^2 \quad (1)$$

The soil positive pressure on the rod cone face F_{p_n}(kN) is:

$$F_{p_n} = \frac{\pi R^2}{\sin\alpha} p_n \quad (2)$$

The soil frictional force on the rod cone face F_n (kN) is:

$$F_n = \frac{\mu\pi R^2}{\sin\alpha} p_n \quad (3)$$

Combine the results of Equations (1)-(3), the axial resistance on the insertion rod F_F (kN) will be:

$$F_F = F_f + F_{p_n}\sin\alpha + F_n\cos\alpha = \mu\pi RK_0\gamma H^2 + \pi R^2(1+\mu\cot\alpha)p_n \quad (4)$$

The necessary condition to ensure a smooth insertion of the rod

into the soil is that the system external force of the rod (F_w) is higher than the axial resistance on the rod (F_F), that is:

$$F_w > F_F = \mu\pi R K_0 \gamma H^2 + \pi R^2 (1 + \mu\cot\alpha) p_n \quad (5)$$

where, K_0 is the earth pressure coefficient at rest, which is set as 1; γ is the soil weight (bulk density), kN/m^3, which is set as 20.58; $2R$ is the cylinder diameter of the insertion rod, mm; H is the insertion depth of the rod cylinder face, mm; 2α is the insertion cone angle of the rod, (°); μ is the relative sliding friction coefficient between rod and soil, which is set as 0.51.

The objective of optimizing the insertion rod is to minimize the soil resistance. The above force analysis showed that the soil friction on the rod is concerned not only with soil parameters, but also with three key structural parameters: rod diameter ($2R$), insertion cone angle (2α), and insertion depth (H).

Based on the settings of soil parameters in literature[18,19] and the calculation method of the positive pressure on the cone face p_n provided in literature[20], the simplified positive pressure on the cone face of the insertion rod p_n (kPa) is:

$$p_n = 412.251\tan\alpha + 249.356 \quad (6)$$

According to Equation (4), the deeper the insertion, the higher the soil resistance on the rod. So the maximum insertion depth designed for the proposed machine is 600 mm to meet the depth requirements of most of fruit trees for subsoiling and fertilizing. Substitute related soil parameters and simplified Equation (6) into Equation (4), the function expression of the axial resistance of the insertion rod will be:

$$F_F = (412.251\tan\alpha + 127.172\cot\alpha + 459.604)\pi R^2 + 11.870R \quad (7)$$

Use Matlab to make the response surface of Equation (7) for the axial resistance of the soil insertion rod (Figure 5).

As shown in Figure 6, the axial resistance F_F increased with the rod radius R in a rising parabolic trend, so the rod diameter should be appropriate (not too large). To realize a good passing of gas fertilizer through the inner cavity of the insertion rod and meet the requirements of rapid injection, the rod diameter $2R$ (outer diameter) was set as 30-40 mm and the inner cavity diameter was set as 20-30 mm, as verified by preliminary tests[10]. When the function $f(\alpha)$=412.251tanα+127.172cotα has the minimum result, the axial resistance of the rod F_F will get the minimum value. Take the derivative of $f(\alpha)$ and a minimum $f(\alpha)$ was got when α=29.05° (α=30° after round off), so the cone angle of the rod was 60°. As the cone angle was set as 60°, and the rod diameter $2R$ was set as 30-40 mm, the axial resistance of the rod F_F would be 0.8526-1.3966 kN. Therefore, the system external force should be larger than this range to meet insertion requirements.

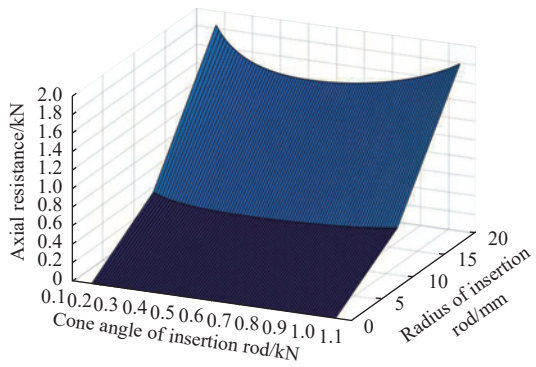

Figure 6 Axial resistance response surface of soil insertion rod

4.2 Simulation analysis of rod insertion process

As a component directly contacting with the soil, the working mode of insertion rod is vertical linear movement. According to the above force analysis, the working of the insertion rod is mainly affected by the axial resistance. To better understand the dynamic behaviors of soil during insertion process and obtain the change law of the axial resistance imposed on the rod, a finite element analysis simulation software LS-DYNA was used to simulate the insertion process of the rod, thus revealing the soil disturbance state caused by the insertion rod, understanding the change law of soil stress, and obtaining the variation characteristics of axial resistance under soil action.

Establish an insertion rod model and a soil model using Solidworks 2016 software, set the distance between the rod model and the soil model as 0, and save in IGS format. Simulate a soil insertion process of the rod to shorten the simulation operation time. With consideration of the simulation accuracy and the actual working conditions of the insertion rod, the rod diameter was set as 30 mm, the insertion speed as 0.08 m/s, the maximum insertion depth as 600 mm, and the soil size as 300 mm×300 mm×700 mm, and we selected MAT_147 from LS-DYNA material base for the soil material to make the constitutive model for the soil simulation[21,22]. This model applied the modified Drucker-Prager yield criterion[23,24].

The soil grid was divided by mapping method. The number of nodes divided by the whole finite element model was 107 624 and the number of elements was 96 376. The simulation parameters are listed as Table 2.

Table 2 Values of the simulation parameters

Item	Parameter	Value
Soil	Density of soil/kg·m^{-3}	2000
	Relative density of soil grains/kg·m^{-3}	2.74
	Soil volume modulus/Pa	3.5×10^8
	Modulus of shear/Pa	2.8×10^8
	Angle of friction/Rad	0.436
	Content of water/%	16
	Eccentricity of soil/%	0.7
	Force of cohesion/MPa	0.022
Insertion rod (65Mn steel)	Density 65Mn steel/kg·m^{-3}	7850
	Elastic modulus 65Mn steel/Pa	2.06×10^{11}
	Poisson's ratio 65Mn steel	0.3

The rod insertion process and soil stress changes are shown as Figure 7. The two sets of diagrams corresponding to three different time points (insertion depth) are the contour maps of the insertion process and related soil stress, respectively. When the rod cone inserts the soil to the depth of 1.2 cm (0.15 s), there is a small range of disturbed soil, as shown in Figure 7a; as the insertion goes deeper, the soil disturbance became fierce with enlarged disturbance volume. Figure 7b shows the soil disturbance at 3.48 s when the depth is 27.8 cm; Figure 7c shows the soil disturbance at 6.90 s when the depth is 55.2 cm. Figure 7 also shows that the cone face of the rod received constant effect from the soil during the insertion process. The soil stress mainly acted around the cone face, and seldom acted on the cylinder face and even invalid as the rod goes deeper. Therefore, it is important to improve the hardness and wear resistance of the cone head of the insertion rod, such as using chrome plated surface.

Figure 8 shows the axial resistance diagram of 30 mm diameter insertion rod subjected to soil action during insertion. As shown, the

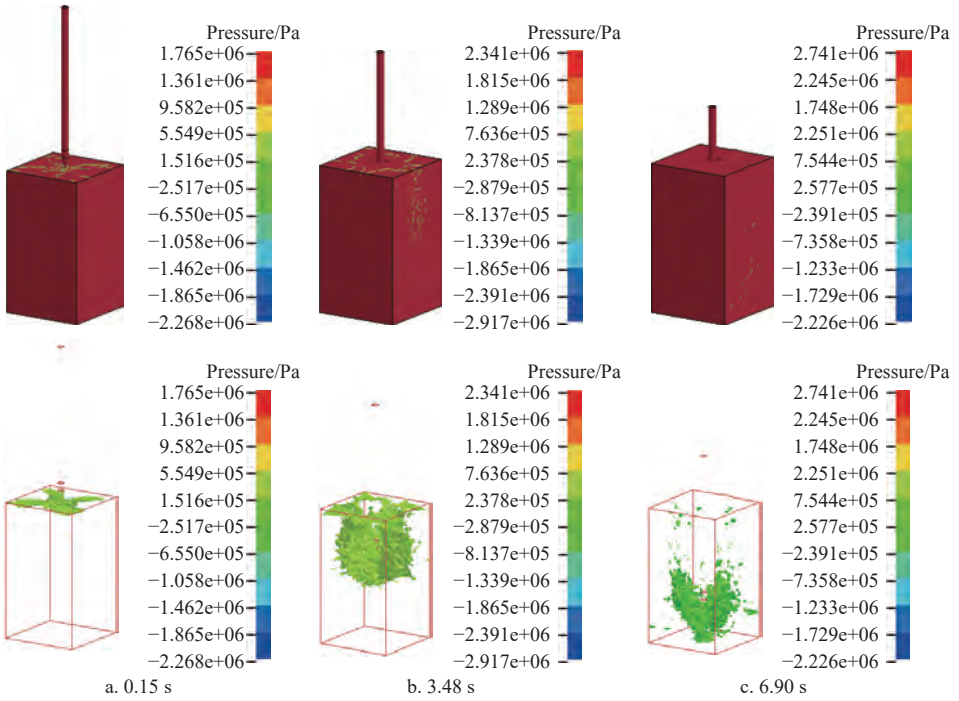

a. 0.15 s b. 3.48 s c. 6.90 s

Figure 7 The process of insertion rod into soil and the change of soil stress

average axial resistance fluctuated at 0.8 kN, which is close to the result (0.8526 kN) of the force analysis on 30 mm diameter insertion rod, indicating that the simulated value is basically the same as the theoretical value.

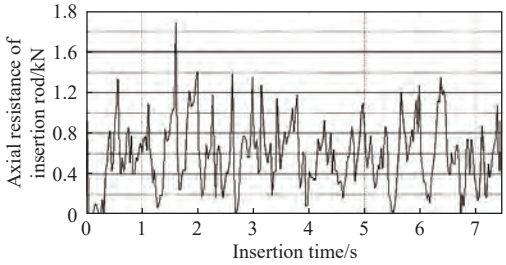

Figure 8 The axial resistance diagram of 30 mm diameter insertion rod subjected to soil action during inserting

5 Insertion performance tests and parameter optimization

5.1 Test conditions

The tests were conducted in the greenhouse of Beiyuan New District of Shihezi University. As shown in Figure 9a, the indoor temperature was 20.5°C and the air humidity was 60.9%. The area of the test field was 16 m×5 m with flat terrain. The soil was mainly clay. The average water content was 14%. The soil was strong in hardness. The harden layer was 30-40 cm thick, and the soil hardness can reach or even exceed 4 MPa. To facilitate the test, three insertion test areas (test points) were designated. The size of each test area was 1.5 m×4.5 m, as shown in Figure 9b.

Test instruments are listed in Table 3.

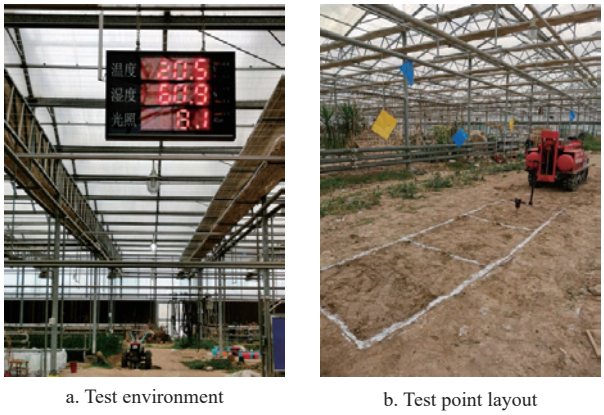

a. Test environment b. Test point layout

Figure 9 The test greenhouse

Table 3 Test instruments

No.	Name	Brand/model	Remarks
1	Gas explosion subsoiling and fertilizing machine	3SQ-600 type	Insertion depth, 600 mm
2	Paperless recorder	Sinomeasure	4-way
3	Laptop	Asus	I7-8550Umemory, 16GB
4	Pressure sensor	Sinomeasure	35 MPa
5	Multimeter	BEST	9205M
6	Soil hardness tester	TJSD-750 type	Precision: ±0.5%
7	Soil moisture meter	TZS-Ⅰ type	Error: ≤3%

Soil hardness is an important indicator to show the physical properties of soil, which is closely related to the soil texture and water content[25]. Higher hardness means higher bearing capacity and tillage resistance of soil as well as higher injection resistance to the rod of insertion device. This paper tested the soil hardness of the test field using TJSD-750 type soil firmness tester. The test results of each area were presented in Figure 10. As shown, the change trends of the three test points were basically the same, indicating

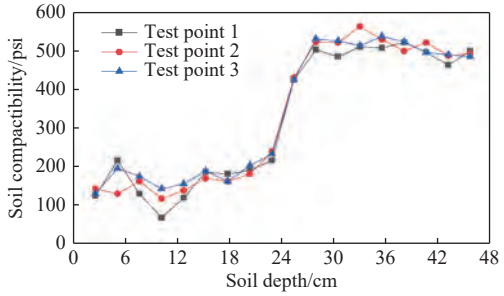

Figure 10 Test results of soil hardness

that the physical properties of each soil layer were relatively uniform. So it can be regarded that each test point has the same soil condition and same insertion resistance at the same soil layer of different test points.

5.2 Test factors

The working parameters and structural parameters of the soil insertion device have certain effect on the insertion performance of gas explosion subsoiling and fertilizing machine under certain soil conditions. A reasonable combination of parameters can keep the pressure of the hydraulic cylinder in an allowable range and avoid the impact from excessive pressure. Engine speed also has effect on the flow rate of the hydraulic pump, thus affecting the speed of the hydraulic cylinder. So engine speed is also a factor to be considered in the test. The engine speed is adjusted by the throttle control handle, and the engine speed can be changed by adjusting the position of the handle to achieve growth or deceleration; At the same time, the change of engine speed can be observed through the tachometer. When it is adjusted to the set target value, it is the proper position of the handle.

In addition, insertion rods with different diameters would receive different soil resistances, and different working time would lead to different insertion depths. Therefore, rod diameter and insertion time are another two factors to be considered.

5.3 Test indicators and test methods

Test indicators: insertion depth is an important indicator for the working quality of gas explosion subsoiling and fertilizing machine; cylinder pressure is an important indicator to show the working condition of the machine.

The cylinder pressure test is shown as Figure 11. During the insertion test at each test point, use paperless recorder to measure the real-time cylinder pressure and save the data. After insertion, use a steel tape to measure the insertion depth and record the results.

Figure 11 Cylinder pressure test

5.4 Test scheme

In order to investigate the impacts of the three parameters (engine speed, rod diameter and insertion time) on the insertion depth and cylinder pressure of the hydraulic insertion device of gas explosion subsoiling and fertilizing machine during the insertion process, this study adopted Box-Behnken central combination test method in attempt to seek the best working condition for insertion. Box-Behnken test design is a multi-factor three-level test design method of response surface method (RSM). This test design can reduce times of tests, improve test efficiency and lower test costs. One of its remarkable advantages is that it uses nonlinear fitting model and has high accuracy. Based on the Box-Behnken test design, this test set the engine speed (X_1), the rod diameter (X_2) and insertion time (X_3) as the independent variables, set the insertion depth (Y_1) and cylinder pressure (Y_2) as the response value, and identify the three-factor and three-level test factors and coding levels, as shown in Table 4.

Table 4 test factors and coding level

Test factors	Coding level		
	–1	0	1
engine speed X_1/(r·min^{-1})	1000	1400	1800
Rod diameter X_2/mm	30	35	40
Insertion time X_3/s	6	8	10

Under the given conditions of Box-Behnken test design, test scheme was established using Design-Expert (V8.0.6.1) software, and tests were carried out by number. Each set of tests were repeated three times. Take the average value as the response value of the insertion depth and cylinder pressure. The test scheme and test results are listed in Table 5.

Table 5 Test scheme and test results

Number	Level of factor			Response value	
	X_1/(r·min^{-1})	X_2/cm	X_3/s	Insertion depth Y_1/cm	Cylinder pressure Y_2/MPa
1	–1	0	1	54	28.4
2	0	0	0	52	29.5
3	0	1	–1	27	31.0
4	1	0	1	61	30.1
5	0	–1	1	62	30.2
6	0	0	0	56	30.8
7	–1	0	–1	8	8.0
8	0	0	0	52	30.5
9	0	–1	–1	36	20.7
10	0	0	0	50	29.2
11	1	0	–1	60	23.3
12	–1	1	0	17	27.2
13	1	1	0	61	31.0
14	1	–1	0	60	31.2
15	0	0	0	50	29.9
16	0	1	1	42	28.6
17	–1	–1	0	25	20.8

5.5 Analysis of test results

5.5.1 Regression equation of insertion depth

Quadratic polynomial regression fitting was performed using the test data in Table 5 to establish the multiple quadratic polynomial regression equations between the engine speed (X_1), rod diameter (X_2), insertion time (X_3) and the insertion depth (Y_1). According to the variance analysis of insertion depth (Table 6), the significance of the established regression equation model of insertion depth (Y_1) was $p<0.0001$, indicating an extremely high level of significance of the model; the goodness of fit was $R^2=0.9659$, indicating a good fitness of the model. The correction coefficient Adj $R^2=0.9304$, and the predicted value was highly correlated with the test value. So this model can be used for the analysis and prediction of the insertion depth (Y_1). The lack of fit was $p=0.0526>0.05$, indicating a small effect of unknown factors on the test results. According to significance tests, the F value of this model was 24.76, and the regression equation of the insertion depth (Y_1) was as follows:

$$Y_1 = 52.00 + 17.25X_1 - 4.50X_2 + 11.00X_3 + 2.25X_1X_2 - 11.25X_1X_3 - 2.75X_2X_3 - 3.63X_1^2 - 7.62X_2^2 - 2.63X_3^2 \quad (8)$$

5.5.2 Analysis of the impact of test factors on the insertion depth

According to Table 6 analysis, the impacts of the model linear

Table 6 Analysis of variance for multiple quadratic polynomial regression equations with insertion depth

Source of variation	SS	df	MS	F	p
X_1	2380.50	1	2380.50	119.88	<0.0001**
X_2	162.00	1	162.00	8.16	0.0245*
X_3	968.00	1	968.00	48.75	0.0002**
X_1X_2	20.25	1	20.25	1.02	0.3462
X_1X_3	506.25	1	506.25	25.49	0.0015**
X_2X_3	30.25	1	30.25	1.52	0.2569
X_1^2	55.33	1	55.33	2.79	0.1390
X_2^2	244.80	1	244.80	12.33	0.0098**
X_3^2	29.01	1	29.01	1.46	0.2660
Model	4425.24	9	491.69	24.76	0.0002**
Residual	139.00	7	19.86		
Lack of fit	115.00	3	38.33	6.39	0.0526
Error	24.00	4	6.00		
Total	4564.24	16			
R^2	0.9659				
AdjR^2	0.9304				

Note: SS is the quadratic sum; df is the degree of freedom; MS is the mean value; * means significant (p<0.05); ** means extremely significant (p<0.01).

terms of engine speed (X_1) and insertion time (X_3), quadratic term (X_2^2), the cross-term engine speed and insertion time (X_1X_3) on the insertion depth were extremely significant, and the impact of the rod diameter (X_2) on the response value was significant, indicating an interactive effect between the test factors. The significance levels of the impacts of the test factors on the insertion depth from high to low in order were: engine speed (X_1) > insertion time (X_3) > rod diameter (X_2).

Set one of the three test factors (engine revolution, insertion time and rod diameter) as the constant and the other two as the independent variable to draw a 3D response surface diagram and related contour diagram of the independent variable and response value (insertion depth), as shown in Figure 12.

According to Figure 12, the contour lines between engine speed (X_1) and insertion time (X_3) were close when the rod diameter (X_2) was at zero level, indicating an extremely significant interactive effect between the engine speed and insertion time. The insertion depth increased significantly with the increase of the engine speed and increased gradually with the insertion time.

Reasons: the hydraulic pump controls the flow of hydraulic oil based on the engine speed. The higher the engine speed, the larger flow of the hydraulic pump and the hydraulic cylinder, leading to faster movement of the cylinder piston pole and the insertion rod and larger insertion depth. Therefore, under the condition of the same rod diameter and insertion time, the insertion depth would increase with the increase of the engine speed. Under the same rod diameter and engine sped, the longer the insertion time, the deeper the insertion, which indicated that the insertion depth increases with the increase of insertion time.

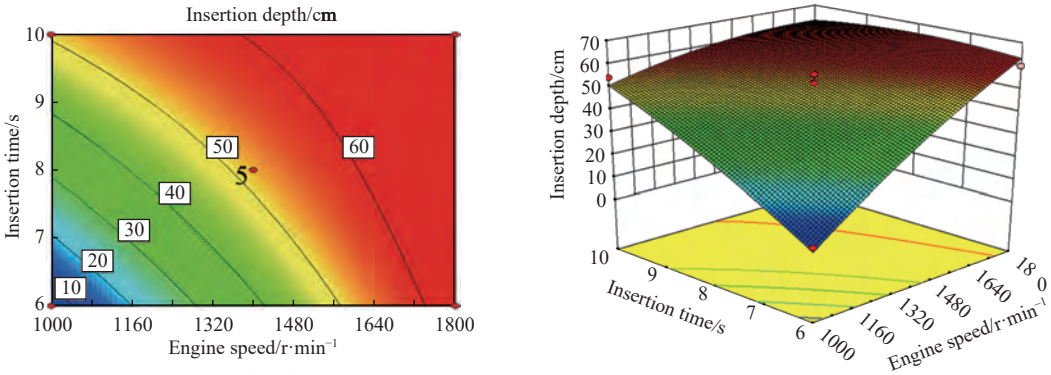

a. Contour line diagram

b. Response surface diagram

Figure 12 Contour and response surface diagram of engine speed and insertion time to insertion depth

One of the optimization objectives of the hydraulic insertion device is to realize a maximum insertion depth. Take the maximum value of insertion depth in Design-Expert (V8.0.6.1) and we get the optimal working parameters of the hydraulic insertion device as follows: engine speed, 1452 r/min; rod diameter, 32 mm; insertion time, 8 s. Under these parameters, the theoretical insertion depth of the hydraulic insertion device was 60 cm.

5.5.3 Regression equation of cylinder pressure

According to the variance analysis of cylinder pressure (Table 7), the significance of the established regression equation model of cylinder pressure (Y_2) was p<0.0001, indicating an extremely high level of significance of the model; the goodness of fit was R^2=0.9971, indicating a good fitness of the model. The correction coefficient Adj R^2=0.9908 and the predicted value were highly correlated with the test value. So this model can be used for the analysis and prediction of the cylinder pressure (Y_2). The lack of fit was p=0.2471>0.05, indicating a small effect of the unknown factors on the test results. According to significance tests, the F value of this model was 158.33, and the regression equation of the cylinder pressure (Y_2) was as follows:

Table 7 Analysis of variance of multiple quadratic polynomial regression equation for cylinder pressure

Source of variation	SS	df	MS	F	p
X_1	1.16	1	1.16	267.36	<0.0001**
X_2	0.28	1	0.28	65.35	0.0005**
X_3	0.13	1	0.13	30.31	0.0027**
X_1X_2	0.11	1	0.11	26.03	0.0038**
X_1X_3	0.85	1	0.85	195.07	<0.0001**
X_2X_3	0.34	1	0.34	78.16	0.0003**
X_1^2	0.79	1	0.79	181.34	<0.0001**
X_2^2	0.15	1	0.15	34.93	0.0020**
X_3^2	0.76	1	0.76	174.83	<0.0001**
Model	7.57	11	0.69	158.33	<0.0001**
Residual	0.022	5	0.004 346		
Lack of fit	0.0068	1	0.0068	1.83	0.2471
Error	0.015	4	0.003 724		
Total	7.59	16			
R^2	0.9971				
AdjR^2	0.9908				

Note: SS is the quadratic sum; df is the degree of freedom; MS is the mean value; * means significant (p<0.05); ** means extremely significant (p<0.01).

$$Y_2 = 5.48 + 0.54X_1 + 0.19X_2 + 0.18X_3 - 0.17X_1X_2 - 0.46X_1X_3 - 0.29X_2X_3 - 0.43X_1^2 + 0.19X_2^2 - 0.42X_3^2 + 0.61X_1^2X_3 - 0.19X_1X_2^2 \quad (9)$$

5.5.4 Analysis of the impact of test factors on cylinder pressure

According to Table 7, the impacts of the model linear terms of engine speed (X_1), rod diameter (X_2), insertion time (X_3), quadratic terms (X_1^2) (X_2^2) (X_3^2), and cross terms (X_1X_2) (X_1X_3) (X_2X_3) on the cylinder pressure were extremely significant, and all the test factors have interactive effects with each other. The significance levels of the impacts of the test factors on the cylinder pressure are in a descending order as engine speed (X_1) > rod diameter (X_2) > insertion time (X_3). The 2D contour and 3D response surface drawn based on quadratic polynomial regression equation (9) are shown in Figure 13.

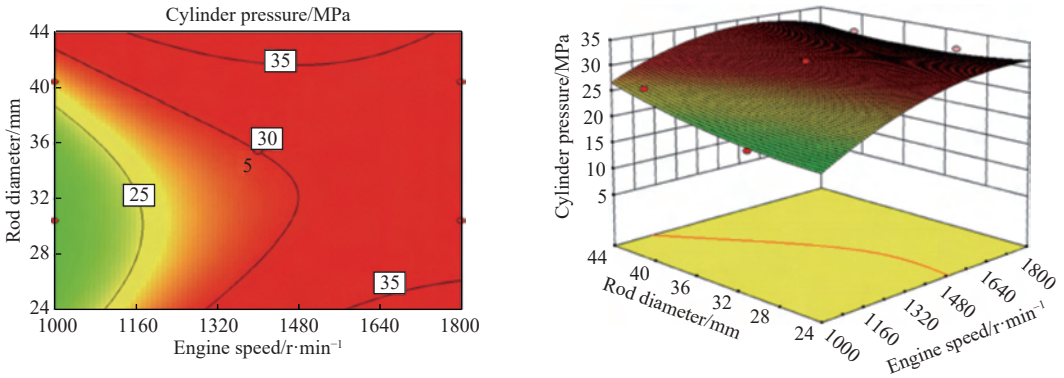

a. Contour and response surface diagram of engine speed and rod diameter to cylinder pressure

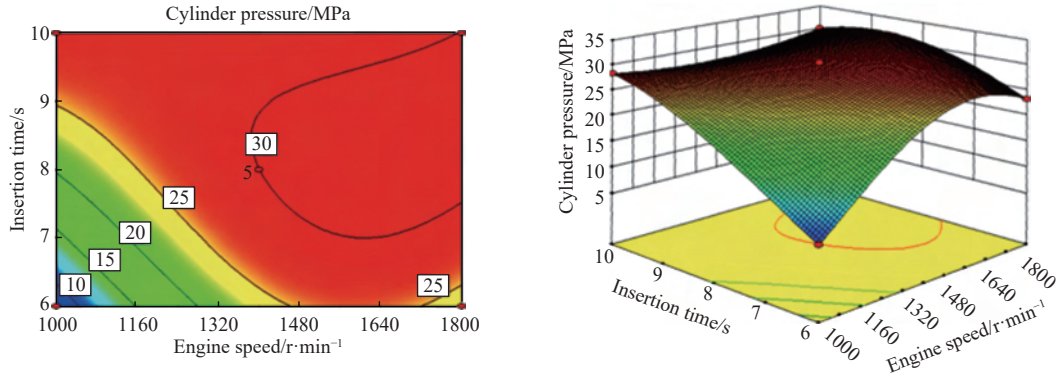

b. Contour and response surface diagram of engine speed and insertion time to cylinder pressure

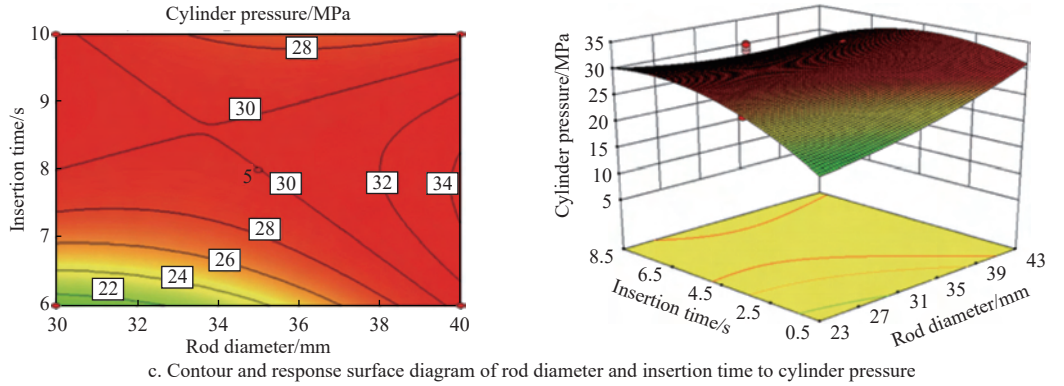

c. Contour and response surface diagram of rod diameter and insertion time to cylinder pressure

Figure 13 Contour and response surface diagram of cylinder pressure

Under certain engine speed, the cylinder pressure of the hydraulic insertion device increased with the increase of the rod size and insertion time. The reason is that, according to Equation (4), the larger the rod diameter, the larger the soil resistance and load on the insertion rod, and the higher the cylinder pressure. With the increase of insertion time and insertion depth, the insertion rod would have larger soil resistance and the cylinder pressure would increase.

Under certain rod diameter or insertion time, the cylinder pressure of the hydraulic insertion device first increased and then decreased with the increase of engine speed. The reason is that the higher the engine speed, the faster the movement of the cylinder piston pole and the deeper the insertion in a certain time. According to Equation (4), the increase of soil resistance on the insertion rod would lead to the increase of the cylinder pressure; the larger the rod diameter, the larger the soil resistance and load on the insertion rod, and the larger the cylinder pressure; when the cylinder pressure exceeds the rated pressure of the overflow valve, the overflow valve would open to release pressure and the cylinder pressure would fall down and maintain in a given pressure.

After optimization of the regression model through Design-

Expert (V8.0.6.1), the following optimal working parameters can be obtained to reduce the cylinder pressure of the hydraulic insertion device: engine speed, 1200 r/min; rod diameter, 30 mm; insertion time, 6 s. Under these conditions, the theoretical value of the cylinder pressure was 8 MPa.

5.6 Parameter optimization and verification

5.6.1 Parameter optimization

To ensure the working quality and improve the efficiency of hydraulic soil insertion device of gas explosion subsoiling and fertilizing machine, an optimal analysis of the structural and working parameters taking larger insertion depth (Y_1) and smaller cylinder pressure (Y_2) as the optimization goal was performed. Then Design-Expert V8.0.6.1 software was applied for the optimal analysis on the regression model established for the two indicators of insertion depth and cylinder pressure. The constraints include: (1) objective function: Y_1[max]; Y_2[min]; (2) influence factor constraints: $X_1 \in [-1,1]$ (engine speed, 1400-1600 r/min); $X_2 \in [-1,1]$ (rod diameter, 30-40 mm); $X_3 \in [-1,1]$ (insertion time, 6-8 s). The optimal combination of influencing factors was obtained as Figure 14 after optimization. The response objective function can cover the region when the insertion time is at 0 level (8 s). Use Design-Expert (V8.0.6.1) to select the combination with the highest satisfaction as the optimal parameters combination, which is: engine speed, 1450 r/min; rod diameter, 32 mm; insertion time, 8 s. The insertion depth predicated by the model was 44.434 cm and the cylinder pressure was 23.085 MPa.

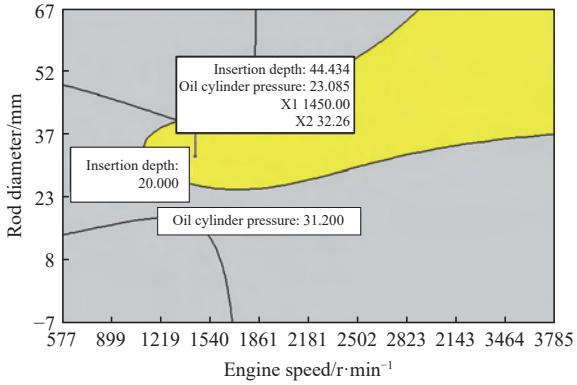

Figure 14 Parameter optimization analysis diagram

5.6.2 Verification tests

To verify the accuracy of the optimization results, verification tests were conducted on the hydraulic soil insertion device using the above-mentioned optimal parameters combination: engine speed, 1450 r/min; rod diameter, 32 mm; insertion time, 8 s. The verification tests (Figure 15) were repeated 5 times, and the prototype and test site were shown. Take the average value of the five repeated verification tests at each test point. The verification results were listed in Table 8.

When operated with above working parameters, the actual test value is close to the model predicted value. Hence, the established regression model can reflect the working parameters of insertion depth and cylinder pressure very well. Figure 16 shows the observation and measurement of perforating profile of rods with different diameters. It was found that the hydraulic insertion device can realize a stable working quality, good insertion quality and high working efficiency using the above combination of parameters, which can meet the agronomic requirements of rapid insertion and appropriate insertion depth in the test site.

Figure 15 Gas explosion subsoiling and fertilizing machine and test site

Table 8 Results of verification tests

Test point	Insertion depth/cm	Cylinder pressure/MPa
1	44.5	23.3
2	46	24.5
3	45	23.6
Average value (Avg.)	45.167	23.8
Standard deviation (S.D.)	0.764	0.624
Coefficient of variation (C.V.)	0.017	0.026

Note: Avg. is the average value; S.D. is the standard deviation; C.V. is the coefficient of variant.

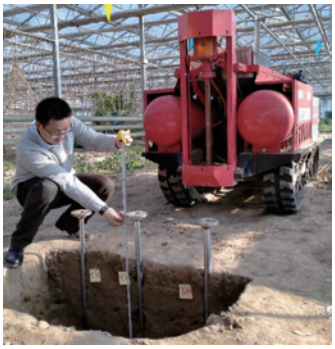

Figure 16 Observation and measurement of perforating profile of rods with different diameters

6 Conclusions

1) Force factors influencing the rod insertion of double-cylinder driven hydraulic insertion device were studied; key parameters equation of insertion resistance were established; force variation rules during the rod insertion were analyzed using LS-DYNA finite element simulation software.

2) Optimal tests of working parameters were conducted based on Box-Behnken optimization design method; influencing rules of the three test factors of engine speed, rod diameter and insertion time on the insertion depth and cylinder pressure were studied; quadratic polynomial regression equations between independent variables and response values.

3) The influences of the test factors on the insertion depth in a descending order were: engine speed > insertion time > rod diameter; the engine speed and insertion time have extremely significant effects on the insertion depth, and the rod diameter has significant effect on the insertion depth; the engine speed has interactive effect with the insertion time.

4) The influences of the test factors on the cylinder pressure were: engine speed > rod diameter > insertion time. The engine speed, rod diameter and insertion time have extremely significant effects on the cylinder pressure; any two of the three factors have

interactive effects on the cylinder pressure.

5) The optimal combination of parameters with full consideration of insertion depth and cylinder pressure was obtained: engine speed, 1450 r/min; rod diameter, 32 mm; insertion time, 8 s. Under this optimal combination working parameters, the insertion depth of the hydraulic insertion device was 44.43 cm and the cylinder pressure was 23.09 MPa. Test verification showed that the hydraulic insertion device using this optimal combination working parameters can meet the agronomic requirements of rapid insertion and appropriate insertion depth in the test site.

Acknowledgements

This research was supported by the National Key Research and Development Project of China (Grant No. 2017YFD0701404), the major science and technology project of Xinjiang Production and Construction Corps (Grant No. 2013AA001-4) and Xinjiang Production and Construction Corps Scientific and technological innovative talent program (Grant No. 2020CB013, 2020CB008).

[References]

[1] Huang X G. Fruit tree nutrition, fertilization and orchard soil management and improvement (Sixth lecture orchard soil management). Fruit Growers' Friend, 2015; 6: 31–32. (in Chinese)

[2] Liu M X, Shi J H, Wang X Y. Study on the relationship between soil main nutrient and yield of Korla Fragrant pear. Soil and Fertilizer Sciences in China, 2018; 1: 140–145. (in Chinese)

[3] Huang J, Zhang Y L, Feng Y Z, Wang Z G, Fu Y B. Spatial variability analysis of root mass of different age walnut trees in southern Xinjiang. Soil and Fertilizer Sciences in China, 2019; 56(9): 1684–1690. (in Chinese)

[4] Kang J M, Li S J, Yang X J, Liu L J, Wang C W, Liu X Q. Design and experiment of ditching blade installed in close planting orchard ditching machinery. Transactions of the CSAM, 2017; 48(2): 68–74. (in Chinese)

[5] Yuan J, Yin R G, Liu G, Liu X M, Mao Z Q. Design and experiment of in-situ fertilizer mixing integrated digging and backfilling planter for fruit tree. Transactions of the CSAM, 2021; 52(2): 110–121. (in Chinese)

[6] Ma C, Qi J T, Kan Z, Chen S J, Meng H W. Operation power consumption and verification tests of a trenching device for orchards in Xinjiang based on discrete element. Int J Agric & Biol Eng, 2021; 14(1): 133–141.

[7] Qi J T, Tian X L, Li Y, Fan X H, Yuan H F, Zhao J L, Jia H L. Design and experiment of a subsoiling variable rate fertilization machine. Int J Agric & Biol Eng, 2020; 13(4): 118–124.

[8] Liu B, Xiao H R, Song Z Y, Mei S. Present state and trends of fertilizing machine in orchard. Journal of Agricultural Mechanization Research, 2017; 11: 263–268. (in Chinese)

[9] Yuan Q C, Xu L M, Xing J J, Duan Z Z, Ma S, Yu C C. Research status and trend of fertilizer deep machine in orchard. Journal of Agricultural Mechanization Research, 2019; 41(6): 258–264. (in Chinese)

[10] Shen C J, Jia S X, Zhang L X, Zhou Y, Li F, Dai Y M, et al. Development of caterpillar self-propelled orchard gas explosion subsoiling and fertilizer machine. Transactions of the CSAE, 2019; 35(17): 1–11. (in Chinese)

[11] Zeng Z L Y, Zeng Z H F. Soil improvement machinery: 201120267100.2. 2012-04-11. (in Chinese)

[12] MAC Engineering Corporation. The original technology for energy conservation.

[13] Xi X B, Zhang R H, Shan X, Jin Y F, Zhang J F. Optimal design and experiment of 3SFBQ-500 type orchard gas explosion subsoiling and fertilizer injection machine. Transactions of the CSAE, 2017; 33(24): 5–43. (in Chinese)

[14] Xi X B. Method and equipment of gas explosion subsoiling & fertilizer injection technology. Yangzhou: Yangzhou University, 2018. (in Chinese)

[15] Zhou W Q, Wang J W, Tang H. Structure optimization of cam executive component and analysis of precisely applying deep-fertilization liquid fertilizer. Int J Agric & Biol Eng, 2019; 12(4): 104–109.

[16] Ma W X, Ge Y, Shen C J, Jia S X, Li F, Dai Y M, et al. Design and kinematic analysis of hydraulic lift hole punching device. Journal of the Gansu Agricultural University, 2020; 55(5): 227–234. (in Chinese)

[17] Yuan J Y, Qian J G, Zhang H M, Liang F Y. Soil mechanics and soil science . Beijing: People's Communications Press, 2001: pp.147–149.

[18] Yu Y T, Jiang J P. Determination of the coefficient of friction of soil, crop seed and various extrudates against steel, cast iron, and wood. Journal of Northeast Agricultural College, 1957; 1: 1–11.

[19] Sun X D, Wang D. Value analysis of soil cohesion. Liaoning Building Materials, 2010; 3: 39–41. (in Chinese)

[20] Liu J. Research on penetrating load characteristics of hammer-driven penetrator for lunar exploration. Harbin: Harbin Institute of Technology, 2016. (in Chinese)

[21] Deng Y J, Zhao Y Q, Xu H, Zhu M X, Zhen X. Finite element modeling of interaction between non-pneumatic mechanical elastic wheel and soil. Proceedings of the Institution of Mechanical Engineers, Part D: Journal of Automobile Engineering, 2019; 233(13): 3293–3304.

[22] Zhou W Q, Sun X B, Liu Z M, Qi X, Jiang D X, Wang J W. Simulation analysis and test of interaction between pricking hole needle body of liquid fertilizer hole applicator and soil. Transactions of the CSAM, 2020; 51(4): 87–94. (in Chinese)

[23] Lewis B A. Manual for LS-DYNA soil material model 147(FHWA-HRT-04-095). Department of Transportation: Federal Highway Administration, USA, 2004.

[24] Reid J D, Coon B A, Lewis B A. Evaluation of LSDYNA soil material model 147 (FHWA-HRT-04-095). Department of Transportation: Federal Highway Administration, USA, 2004.

[25] Chen Y G, Shi Y N. Analysis of physical and mechanical properties of soil. Journal of Agricultural Mechanization Research, 2002; 2: 60–60.